Chemical Engineering and Processing 68 (2013) 7–12

Contents lists available at SciVerse ScienceDirect

Chemical Engineering and Processing: Process Intensification

journal homepage: www.elsevier.com/locate/cep

Gravity-driven thin film flow: The influence of topography and surface tension gradient on rivulet formation

D. Slade [a,*], S. Veremieiev [a], Y.C. Lee [b], P.H. Gaskell [a]

[a] School of Mechanical Engineering, University of Leeds, Leeds, LS2 9JT, UK
[b] Department of Mechanical Engineering, Heriot-Watt University, Edinburgh, EH14 4AS, UK

ARTICLE INFO

Article history:
Received 19 November 2011
Received in revised form 3 July 2012
Accepted 11 July 2012
Available online 20 July 2012

Keywords:
Thin film
Rivulet
Lubrication theory
Marangoni stress
Topography

ABSTRACT

The evolution of an advancing fluid front formed by a gravity-driven thin film flowing down a planar substrate is considered, with particular reference to the presence of Marangoni stresses and/or surface topography. The system is modelled using lubrication theory and solved via an efficient, adaptive multigrid method that incorporates automatic, error-controlled grid refinement/derefinement and time stepping. The detailed three dimensional numerical results obtained reveal that, for the problems investigated, while both of the above features affect the merger of rivulets by either delaying or promoting the same, topography influences the direction of growth.

1. Introduction

Thin film flows over substrate containing heterogeneities in the form of micro-scale topographical irregularities arise in many naturally occuring biological, medical and industrial processes [1]. The resulting complex and interesting fluid dynamics involved, as well as the stability of the advancing front formed by a spreading film, make the topic of rivulet formation in particular both important and fascinating. The observed formation of rivulets on an inclined homogeneous substrate was first reported by Huppert [2], who recorded that the advancing front became unstable leading to the development of periodic rivulets that grew in time. There have been many subsequent investigations, mainly numerical, of the phenomenon; for example Diez and Kondic [3] explored gravity-driven flow on inclined planar and patterned substrates, discovering that the inclination angle affects the shape and length of the rivulet patterns formed. Cazabat et al. [4] investigated experimentally the case of a film driven, in opposition to gravity, by thermal gradients and found that, in a similar way to gravity-driven films, rivulets form at the advancing front – the surface tension gradients present having a large influence on the associated dynamics. Eres et al. [5] developed a model to replicate their experimental set up and predicted the break up of the associated rivulets at low velocities.

Kondic and Diez [6] investigated the affect of small perturbations in the substrate on a stable front; the resulting rivulet formation was found to be very similar to that observed when contact line perturbations are applied to the advancing front. The use of striped substrates in the control of rivulet spacing has also been investigated, Kondic and Diez [7]. Zhao and Marshall [8] modelled the chemical heterogeneity of a substrate by varying the contact angle the fluid makes with it; striped surfaces are reported to provide a means of controlling the wavelength of the emerging rivulets, either widening or decreasing the spacing between them.

The focus of the present work is that of a fully wetting, three dimensional, gravity-driven thin film, encompassing flow on planar substrates and ones containing microscale topographies. Also considered are Marangoni effects, which can arise when thermal gradients are present. The flow behaviour is modelled via lubrication theory; the associated equation set governing the evolving flow is solved accurately using an efficient multigrid methodology, incorporating both error controlled, automatic space and time adaptivity – the first time such flows have been solved in this manner.

2. Problem formulation

The problem of interest is shown schematically in Fig. 1. It consists of a thin fluid film of thickness H, flowing down a substrate (width, W_p, length, L_p) inclined at angle θ to the horizontal; the volumetric flow rate is Q_0 per unit width. The fluid is considered to be incompressible with constant density, ρ, and viscosity, μ, and

* Corresponding author.
E-mail address: mndsl@leeds.ac.uk (D. Slade).

0255-2701/$ – see front matter © 2012 Elsevier B.V. All rights reserved.
http://dx.doi.org/10.1016/j.cep.2012.07.003

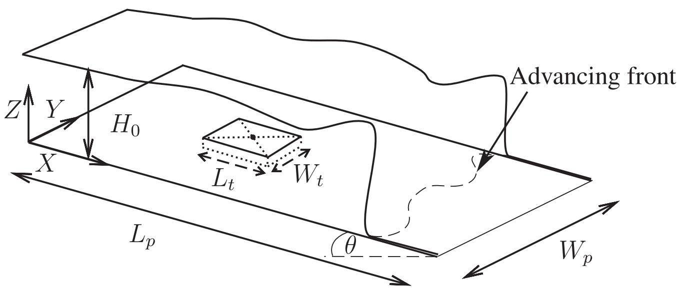

Fig. 1. Schematic diagram of rivulet flow down an inclined planar substrate containing rectangular topography (height/depth S_0, width, W_t, and length, L_t).

variable surface tension, σ, given by $\sigma = \sigma_0\tilde{\sigma} = \sigma_0 + \tau X$ with σ_0 the value of surface tension at $X = 0$ and $\tau \left(= \partial\sigma/\partial X\right)$ a constant surface tension gradient [4]. The film is considered to be fully wetting; a precursor film of thickness, H^*, located ahead of the advancing front, alleviates the singularity associated with the attendant contact line [6,8,9]. The long-wave approximation is invoked on the assumption that the asymptotic film thickness, H_0, is small compared to the capillary length, $L_0 = H_0/(6Ca)^{1/3}$, where $Ca = \mu U_0/\sigma_0 \sim O\left(\epsilon^3\right) \ll 1$ is the capillary number, that is $H_0/L_0 = \epsilon \ll 1$; the characteristic velocity $U_0 = 3Q_0/2H_0$. In which case, together with the introduction of the following scalings [10]:

$$(x, y) = \frac{(X, Y)}{L_0}, \quad z = \frac{Z}{H_0}, \quad h(x, y, t) = \frac{H(X, Y, T)}{H_0},$$
$$t = \frac{U_0 T}{L_0}, \quad s(x, y) = \frac{S(X, Y)}{H_0}$$
$$p(x, y, z, t) = \frac{2P(X, Y, Z, T)}{\rho g L_0 \sin\theta},$$
$$(u, v, w) = \left(\frac{U}{U_0}, \frac{V}{U_0}, \frac{W}{\epsilon U_0}\right), \quad h^* = \frac{H^*}{H_0},$$

the Navier–Stokes and continuity equations, for no slip at the substrate together with the usual free-surface stress and kinematic boundary conditions [11], reduce to the following coupled equation set:

$$\frac{\partial h}{\partial t} = \frac{\partial}{\partial x}\left[\frac{h^3}{3}\left(\frac{\partial p}{\partial x} - 2\right) - \frac{\tilde{\tau} h^2}{2}\right] + \frac{\partial}{\partial y}\left[\frac{h^3}{3}\left(\frac{\partial p}{\partial y}\right)\right], \tag{1}$$

$$p = -\frac{\epsilon^3}{Ca}\hat{\sigma}\nabla^2(h + s) + 2\epsilon(h + s - z)\cot\theta, \tag{2}$$

where $h, p, \tilde{\tau}\ (= H_0\tau\ /\ \mu U_0)$ and s are the dimensionless film height, pressure, constant surface tension gradient and topography height/depth, respectively. The topography, $s(x, y)$, with height (depth) $s_0 = S_0/H_0 > 0$ ($s_0 < 0$), length $l_t = L_t/L_0$ and width $w_t = W_t/L_0$, defined using arctangent functions [12], takes the form:

$$s(x, y) = \frac{s_0}{b_0}\left[\tan^{-1}\left(\frac{x - x_t - \frac{l_t}{2}}{\gamma l_t}\right) + \tan^{-1}\left(\frac{x_t - x - \frac{l_t}{2}}{\gamma l_t}\right)\right]$$
$$\times \left[\tan^{-1}\left(\frac{y - y_t - \frac{w_t}{2}}{\gamma w_t}\right) + \tan^{-1}\left(\frac{y_t - y - \frac{w_t}{2}}{\gamma w_t}\right)\right] \tag{3}$$

with the centre of the topography at (x_t, y_t). The steepness of the topography is controlled by γ with:

$$b_0 = 4\left[\tan^{-1}\left(\frac{1}{2\gamma}\right)\right]^2. \tag{4}$$

When topographies are present, they are restricted to simple square peak and trench features with $\gamma = 0.01$.

At the upstream boundary a fully developed film thickness is prescribed ($h = 1$) while the downstream boundary is set such that $h(l_p, y) = h^*$ with zero flux conditions defined for h and p at the other boundaries, namely:

$$\left.\frac{\partial h}{\partial x}\right|_{x=0} = \left.\frac{\partial p}{\partial x}\right|_{x=0} = \left.\frac{\partial h}{\partial x}\right|_{x=l_p} = \left.\frac{\partial p}{\partial x}\right|_{x=l_p} = 0,$$

$$\left.\frac{\partial p}{\partial y}\right|_{y=0} = \left.\frac{\partial p}{\partial y}\right|_{y=w_p} = \left.\frac{\partial h}{\partial y}\right|_{y=0} = \left.\frac{\partial h}{\partial y}\right|_{y=w_p} = 0.$$

where $l_p = L_p/L_0$ and $w_p = W_p/L_0$. The initial film profile consists of a front perturbed with a superposition of N modes with random length, $l_j \in [-0.2, 0.2]$, and differing wavelength, $\lambda_{0,j}$, as in [6] via:

$$h(x, y) = 0.5\left\{1 + h^* - (1 - h^*)\tanh\left[\frac{\left(x - x_f(y)\right)}{\delta}\right]\right\}, \tag{5}$$

$$x_f(y) = x_u - \sum_{j=1}^{N} l_j \cos\left(2\pi y/\lambda_{0,j}\right), \tag{6}$$

where x_u is the position of the slope of the unperturbed front, δ is the steepness of the profile (taken here to be 0.01) and $\lambda_{0,j} = 2w_p/j$ for $j = 1, \ldots, N$. The results are independent of the initial condition provided N is sufficiently large; a value of $N = 50$ is found to be adequate.

3. Method of solution

3.1. Difference equations

Discretising Eqs. (1) and (2) using second order central-differencing [10], remembering that $\tilde{\tau}$ is constant, leads to the following corresponding finite-difference analogues:

$$\begin{aligned}\frac{\partial h_{i,j}}{\partial t} = \frac{1}{\Delta^2}&\left[\frac{h^3}{3}\Big|_{i+\frac{1}{2},j}\left(p_{i+1,j} - p_{i,j}\right) - \frac{h^3}{3}\Big|_{i-\frac{1}{2},j}\left(p_{i,j} - p_{i-1,j}\right)\right.\\ &\left.+\frac{h^3}{3}\Big|_{i,j+\frac{1}{2}}\left(p_{i,j+1} - p_{i,j}\right) - \frac{h^3}{3}\Big|_{i,j-\frac{1}{2}}\left(p_{i,j} - p_{i,j-1}\right)\right]\\ &-\frac{\tilde{\tau}}{2\Delta}\left(\frac{h^2|_{i+1,j}}{3} - \frac{h^2|_{i-1,j}}{3}\right) - \frac{2}{\Delta}\left(\frac{h^3}{3}\Big|_{i+\frac{1}{2},j} - \frac{h^3}{3}\Big|_{i-\frac{1}{2},j}\right),\end{aligned} \tag{7}$$

$$\begin{aligned}p_{i,j} + \frac{\epsilon^3\hat{\sigma}}{Ca\Delta^2}&\left[(h_{i+1,j} + s_{i+1,j}) + (h_{i-1,j} + s_{i-1,j}) + (h_{i,j+1} + s_{i,j+1})\right.\\ &\left.+(h_{i,j-1} + s_{i,j-1}) - 4h_{i,j}\right] - 2\epsilon\left(h_{i,j} + s_{i,j}\right)\cot\theta = 0,\end{aligned} \tag{8}$$

defined at all points (i, j) of the computational domain, $\left(0, l_p\right) \times \left(0, w_p\right)$; the prefactors are obtained using linear interpolation between neighbouring grid points and are given by, for example,

$$\frac{h^3}{3}\Big|_{i+\frac{1}{2},j} = \frac{1}{2}\left(\frac{1}{3}h^3_{i+1,j} + \frac{1}{3}h^3_{i,j}\right),$$

and similarly for the other prefactors. The mesh size is denoted by Δ and is taken to be the same in both the x and y directions. The time derivatives are discretised via the implicit, second-order Crank Nicolson method.

3.2. Adaptive multigrid solver

Equations (7) and (8) are solved using an efficient multigrid method employing a combined full approximation storage (FAS) algorithm and full multigrid (FMG) strategy, on successively finer